Academic Platform Journal of Engineering and Science

journal homepage: http://apjes.com/

Composition And Temperature Dependences In Ising-Type Multisegment Nanostructure

*[1] Ersin Kantar
[1] Sorgun Vocational School, Bozok University, 66700 Yozgat, Turkey,
ersin.kantar@bozok.edu.tr,

Research Paper Received Date: 12.01.2018 Accepted Date: 27.07.2018

Abstract

In the present study**,** an Ising-type multisegment nanowire (IMN) with ferromagnetic / non-magnetic segment structure is investigated by means of the effective-field theory (EFT) with correlations. The effects of the composition (p) and temperature (T) on the magnetic hysteresis properties are investigated in detail. The coercive field (H_C) and squareness (M_r /M_S) of the IMN is also derived from hysteresis loops as a function of p and T. In this system, it was found that the p and T have a significant effect on the magnetic behavior. When the obtained theoretical results compare with some experimental works of nanowire in view of hysteresis behaviors, a very good agreement between them is observed.

Keywords: Ising model; Multisegment nanowire; Effective field theory; Hysteresis behavior.

1. INTRODUCTION

In recent years, multicomponent nanostructures have attracted a great interest for their unique physical properties [1-4] and potential applications [5, 6]. Generally, there are two types morphologies in multicomponent nanostructures: radial structures, such as core/shell type, and axial structures, namely segmented type. Multicomponent nanostructures with core/shell structure such as core/shell nanowire and core/shell nanotube have been studied to explain many physical characteristics in nanoparticle magnetism [7-12].

Some studies on hard/soft core/shell nanoparticles are revealing interesting magnetic properties, such as reversible tuning of the blocking temperature [13], improved microwave absorption [14], optimized hyperthermia [15], and enhanced coercivity [16].

Moreover, segmented nanostructures have mainly focused on two segments of nanowires, nanotubes and nanowire/nanotube segment. Magnetic segmented nanowires have been increasing, because of their multifunctional and structural advantages compared to their counterparts, single-component nanowires. Magnetic segmented nanowires consisting of alternating structures of ferromagnetic-ferromagnetic or ferromagnetic-nonmagnetic materials, such as Ni/Cu [17, 18], Ni/Au [19], Co/Cu [20-24], Fe/Cu [25], NiFe/Cu [26], CoNi/Cu [27, 28], FeCoNi/Cu [29], FeGa/Cu [30], Co/Pt [31], Ni/Pt [32], Fe/Pt [33], NiFe/Pt [34], Co/ Au [35] and NiCoCu/Cu [36, 37] have been reported in literature. On the other hand, magnetic segmented nanowires show novel and interesting properties depending on their morphologies. Therefore, their have been also studied to investigate the dependence of geometrical (by the segment thicknesses, wire diameter, and aspect ratio), angular (by the applied field angle) and compositional on the magnetic properties. In this context, composition dependent hysteresis properties on nanostructures such as Co/Ni [38, 39], Co/Cu [40, 41], CoFeCu [42], and NiCoCu [43] have been investigated. It should also be noted that the Ising model is a well-known and has a venerable tradition in the applications to order–disorder systems, such as ferromagnetic or ferroelectric systems, binary alloys, lattice gases and complex fluid.

The model has been also used to understand the magnetic properties of nanostructured systems, due to has an important role in the deeper understanding of behaviors in magnetic systems. In this concept, the magnetic nanowires have been investigated within the various theoretical methods, such as effective-field theory (EFT) with correlations [44-46], mean-field theory (MFT) [47-49], and Monte Carlo (MC) simulations [50]. The dynamic magnetic properties of Ising nanowire systems are also investigated by using the above theoretical methods [51-53].

Although a great amount of the Ising systems have been used to investigate the magnetic properties of nanostructured systems, there has been only a few works where the Ising system is used to investigate magnetic properties of segmented nanostructure [46, 54, 55]. In these works, the hysteresis properties of the mixed spin (1/2-1) [46, 54] and pure spin 1/2 [55] Ising systems were investigated on the segmented nanostructure by using the EFT with correlations. In pure spin 1/2 system, geometry-dependent magnetic properties of Ising-Type segmented nanowire were studied.

*Corresponding author. Sorgun Vocational School, Bozok University, 66700 Yozgat, Turkey Tel: + 90 (354) 502 00 55; Fax: + 90 (354) 502 00 54. E-mail address: ersin.kantar@bozok.edu.tr

Doi: 10.21541/apjes.378426

Therefore, in the present study, the effects of composition and temperature on the magnetic hysteresis behaviors of a pure spin 1/2 segmented nanostructure with ferromagnetic / non-magnetic segments are discussed by means of the EFT with correlations.

2. MODEL AND FORMULATION

The Hamiltonian of the IMN with ferromagnetic (FM) / non-magnetic (NM) segment is given by $H = H_{FM-NM} + H_{FM} + H_{NM}$. In here, H_{FM-NM} (inter-segment interactions), H_{FM} (FM segment interactions) and H_{NM} (NM segment interactions) following as,

$$H_{FM-NM} = -J_{Int}\left(\sum_{\langle kk'\rangle} S_k \sigma_{k'} \xi_{k'} + \sum_{\langle ii'\rangle} S_i \sigma_{i'} \xi_{i'}\right) \tag{1a}$$

$$\begin{aligned} H_{FM} = & -J_S \sum_{\langle ij\rangle} S_i S_j - J_D \sum_{\langle ik\rangle} S_i S_k \\ & - J_W\left(\sum_{\langle kk''\rangle} S_k S_{k''} + \sum_{\langle ii''\rangle} S_i S_{i''}\right) \\ & - h\left(\sum_i S_i + \sum_k S_k + \sum_{i''} S_{i''} + \sum_{k''} S_{k''}\right), \end{aligned} \tag{1b}$$

$$\begin{aligned} H_{NM} = & -J_S \sum_{\langle i'j'\rangle} \sigma_{i'}\sigma_{j'}\xi_{i'}\xi_{j'} - J_D \sum_{\langle i'k'\rangle} \sigma_{i'}\sigma_{k'}\xi_{i'}\xi_{k'} \\ & - J_W\left(\sum_{\langle kk''\rangle} \sigma_k \sigma_{k''}\xi_k \xi_{k''} + \sum_{\langle ii''\rangle} \sigma_i \sigma_{i''}\xi_i \xi_{i''}\right) \\ & - h\left(\sum_{i'} \sigma_{i'}\xi_{i'} + \sum_{k'} \sigma_{k'}\xi_{k'} + \sum_{i''} \sigma_{i''}\xi_{i''} + \sum_{k''} \sigma_{k''}\xi_{k''}\right), \end{aligned} \tag{1c}$$

where <...> denote the summations over all pairs of neighboring spins at the shell surface, between FM and NM segments and between shell surface and core, respectively. h is external magnetic field. The surface shell is coupled to the next shell in the core with an exchange interaction J_W. J_S is the exchange interaction between two nearest-neighbor atoms at the surface shell. The parameter $\xi_\alpha\ (\alpha = i', j', k')$ is a site occupancy number that is 1 or zero, depending on whether the site is occupied or not. Since only the NM segment is diluted in the present system, ξ_α takes unity with a probability p when the site α is occupied by a magnetic atom and takes 0 with a probability (1−p) when the site α on the NM segment is occupied by a NM atom.

Within the framework of the EFT [56], which includes spin–spin correlations resulting from the usage of the van der Waerden identities [57], we can obtain the longitudinal magnetization m_{S1} and m_{S2} at the surface shell and the longitudinal magnetization m_{C1} and m_{C2} at the core. The coupled equations are given by:

$$\begin{aligned} m_{S1} = & \left[\cosh(A) + 2m_{S1}\sinh(A)\right]^2 \\ & \left[\cosh(B) + 2m_{C1}\sinh(B)\right] \\ & \left[p\left(\cosh(C) + 2m_{S2}\sinh(C)\right) + 1 - p\right] \\ & \left[\cosh(D) + 2m_{S1}\sinh(D)\right] F(x+h)\big|_{x=0}, \end{aligned} \tag{2a}$$

$$\begin{aligned} m_{C1} = & \left[\cosh(B) + 2m_{S1}\sinh(B)\right]^6 \\ & \left[p\left(\cosh(C) + 2m_{C2}\sinh(C)\right) + 1 - p\right] \\ & \left[\cosh(D) + 2m_{C1}\sinh(D)\right] F(x+h)\big|_{x=0}, \end{aligned} \tag{2b}$$

$$\begin{aligned} m_{S2} = & \left[p\left(\cosh(A) + 2m_{S2}\sinh(A)\right) + 1 - p\right]^2 \\ & \left[p\left(\cosh(B) + 2m_{C2}\sinh(B)\right) + 1 - p\right] \\ & \left[\cosh(C) + 2m_{S1}\sinh(C)\right] \\ & \left[p\left(\cosh(D) + 2m_{S2}\sinh(D)\right) + 1 - p\right] F(x+h)\big|_{x=0}, \end{aligned} \tag{2c}$$

$$\begin{aligned} m_{C2} = & \left[p\left(\cosh(B) + 2m_{S2}\sinh(B)\right) + 1 - p\right]^6 \\ & \left[\cosh(C) + 2m_{C1}\sinh(C)\right] \\ & \left[p\left(\cosh(D) + 2m_{C2}\sinh(D)\right) + 1 - p\right] F(x+h)\big|_{x=0}, \end{aligned} \tag{2d}$$

Here, the coefficients A, B, C and D are $J_S\nabla$, $J_D\nabla$, $J_{Int}\nabla$ and $J_W\nabla$, respectively. Moreover, $\nabla = \partial/\partial x$ is the differential operator [56]. The $F(x+h)$ function is defined as follow:

$$F(x+h) = \frac{1}{2}\tanh\left[\frac{1}{2}\beta(x+h)\right]. \tag{3}$$

Here, $\beta = 1/k_B T$, T is the absolute temperature and k_B is the Boltzmann constant. By using the definitions of the order parameters in Eqs. (2a)-(2d), the total magnetizations m_T of per site can be defined as $m_T = \dfrac{\left(m_{C1} + p\,m_{C2} + 6\left(m_{S1} + p\,m_{S2}\right)\right)}{7 + 7p}$.

The next section is devoted to these calculations in order to obtain the hysteresis behaviors of the IMN.

3. NUMERICAL RESULTS AND DISCUSSIONS

In numerical calculations, within Ising model framework, EFT with correlation are used to examine the magnetic hysteresis behaviors of IMN with ferromagnetic / non-magnetic segment structure. We investigate the effects of the composition and temperature on the hysteresis behaviors of the system.

3.1. The influence of the temperature on the hysteresis behaviors

In order to investigate temperature dependence of the magnetic hysteresis in the IMN system, a series of hysteresis loops for two regimes ,$T < T_C$ (T=0.1, 0.3, 0.5, 0.7 and 0.9) and $T \geq T_C$ (T=1.1, 1.3 and 1.5), are plotted by using fixed parameters $J_W=J_{Int}=J_D=J_S=1$ and p = 0.1,. 2(a). When the

temperature increases, the area enclosing the single hysteresis loop decreases. if the temperature increases stronger, the single hysteresis loop disappears in the case of $T \geq T_C$, which confirms the disappearance of ferromagnetic properties at vanishing temperature. In this case, the Curie temperature is T_C=1.1. These results are consistent with nanostructure systems within the theoretical [58-61] and experimental [62-64] framework. Magnetic properties of the IMN such as H_C, and M_r /M_S ratio have been also studied at various temperatures between 0.1 and 1.5. From Figs. 2(b) and 2(c), the results show that the H_C, as well as the M_r /M_S, decreases with the increasing temperature.

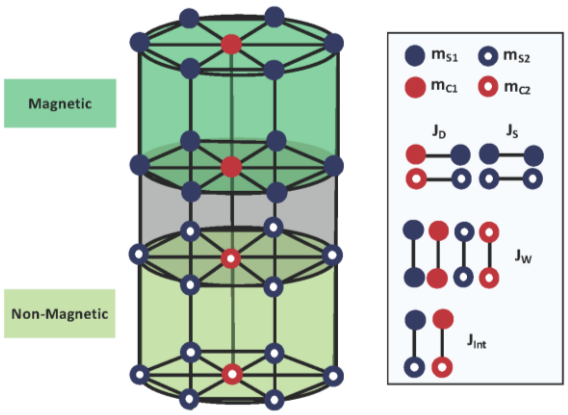

Figure 1. (Color online) Schematic representation of Ising-type multisegment nanowire. The spheres and circles indicate ferromagnetic and non-magnetic atoms, respectively. Moreover, the blue and red colors that shows the location of the surface shell and core magnetic atoms.

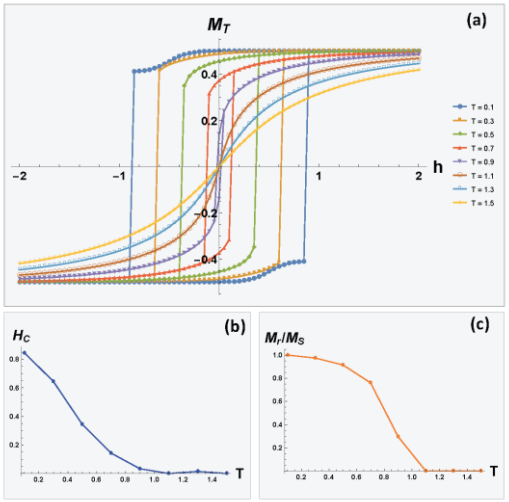

Figure 2. (Color online) Magnetic hysteresis loops of Ising-type multisegment nanowire and the temperature dependence of the coercive field (H_C) and squareness (M_r /M_S) for the fixed values of J_W=J_{Int}=J_D=J_S=1 and p = 0.1. (a) The hysteresis loops for T values ranging from 0.1 to 1.5 (b) The temperature dependence of the coercive field (H_C). (c) The temperature dependence of the squareness (M_r /M_S).

3.2. The influence of the composition on the hysteresis behaviors

Figure 3 shows the compositional dependence of hysteresis behavior within selected six typical p values, namely 0.1, 0.3, 0.5, 0.7, 0.9 and 1.0, in the cases of J_W=J_{Int}=J_D=J_S=1 and T = 0.1. The system only shows a single hysteresis loop behavior. As seen in Figs. 3(a)-(c), with the increase of p, the single hysteresis loop becomes smaller. From Figs. 3(d)-(f), when the values of p is higher than 0.5 values, the single hysteresis loop becomes larger. From Fig. 3(g), the H_C shows there is a small reduction from 0.83 to 0.59 with increasing p values, in addition to this, with higher p values it reaches up to values of around 1.4. Moreover, Mr /Ms, increases with the increasing p values (Fig. 3(h)). Experimentally, in Co/Ni multisegment nanowire [38, 39] has been also seen as similar H_C behavior.

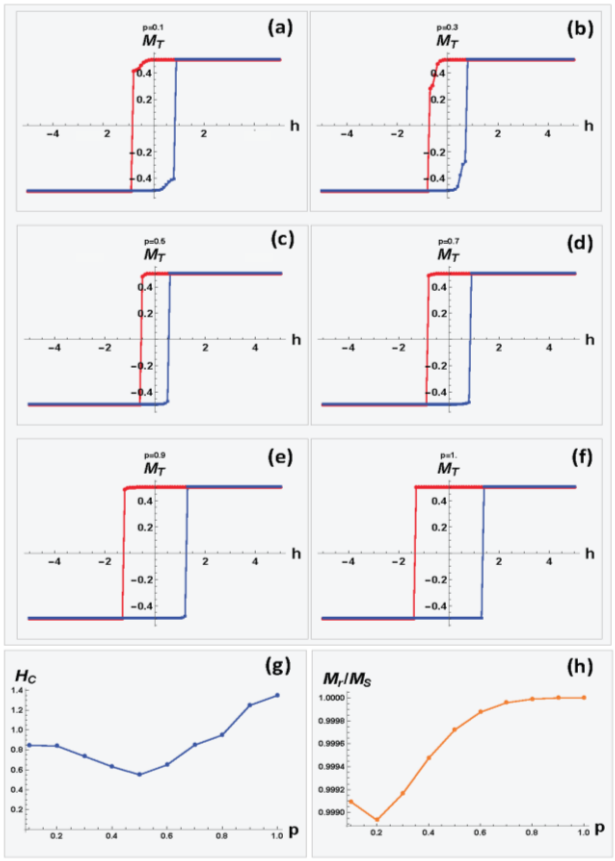

Figure 3. (Color online) The composition dependence of the hysteresis loops, the coercive field (H_C) and squareness (M_r /M_S) for the fixed value of J_W=J_{Int}=J_D=J_S=1 and T = 0.1. (a) In p =0.1, M_T-h curve. (b) In p =0.3, M_T-h curve. (c) In p =0.5, M_T-h curve. (d) In p =0.7, M_T-h curve. (e) In p =0.9, M_T-h curve. (f) In p =1.0, M_T-h curve. (g) The composition dependence of the coercive field (H_C). (h) The composition dependence of the squareness (M_r /M_S).

3.3. Soft/hard magnetic behaviors

In this study, it was also investigated the soft and hard magnetic behaviors of the multisegment Ising nanowire in (p, T) plane, and it was plotted in Fig. 4 for the fixed values of $J_W=J_{Int}=J_D=J_S=1$. It can be seen from Fig. 6 that hard magnetic behaviors may occur in both low and high p with a low T. For high T values, the hard magnetic behaviors start turns to the soft. After certain values of T, system shows paramagnetic behavior.

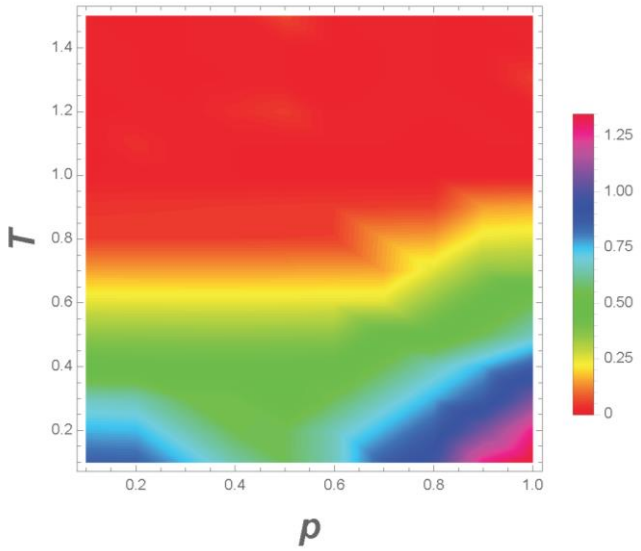

Figure 4. (Color online) The phase diagram in (p, T) plane of the Ising-type multisegment nanowire for the fixed values of $J_W=J_{Int}=J_D=J_S=1$.

4. SUMMARY AND CONCLUSİONS

In this paper, the hysteresis behaviors of a Ising-type multisegment nanowire with ferromagnetic/non-magnetic segment structure is studied by using the framework effective-field theory with correlations. The effect of the temperature and composition on the hysteresis behavior via concerning the M_T-h curves, H_C and M_r /M_S features are investigated.

It was found that when the temperature increases, the area enclosing the single hysteresis loop decreases, and then keep increasing temperature, the hysteresis loops disappear at the critical temperature.

Moreover, the hard magnetic behavior is observed in low p values. Obtaining theoretical results have qualitatively compatible with some experimental works of segmented nanowire.

ACKNOWLEDGEMENTS

I am very grateful to Lecturer Ali Doğantekin who reads the manuscript carefully and corrected numerous English mistakes

REFERENCE

[1] R. Ghosh, and D. Basak, “Electrical and ultraviolet photoresponse properties of quasialigned ZnO nanowires/p-Si heterojunction,” Applied Physics Letters, vol. 90, no. 24, Jun 11, 2007.
[2] S. W. Jung, W. I. Park, G. C. Yi, and M. Kim, “Fabrication and controlled magnetic properties of Ni/ZnO nanorod heterostructures,” Advanced Materials, vol. 15, no. 16, pp. 1358-+, Aug 15, 2003.
[3] J. D. Ye, S. L. Gu, S. M. Zhu, S. M. Liu, Y. D. Zheng, R. Zhang, and Y. Shi, “Fermi-level band filling and band-gap renormalization in Ga-doped ZnO,” Applied Physics Letters, vol. 86, no. 19, May 9, 2005.
[4] J. Luo, Z.P. Huang, Y.G. Zhao, L. Zhang, and J. Zhu, “Arrays of heterojunctions of Ag nanowires and amorphous carbon nanotubes,” Advanced Materials, vol. 16, pp. 1512–1515, 2004.
[5] C. Thelander, T. Martensson, M. T. Bjork, B. J. Ohlsson, M. W. Larsson, L. R. Wallenberg, and L. Samuelson, “Single-electron transistors in heterostructure nanowires,” Applied Physics Letters, vol. 83, no. 10, pp. 2052-2054, Sep 8, 2003.
[6] S. Park, S. W. Chung, and C. A. Mirkin, “Hybrid organic-inorganic, rod-shaped nanoresistors and diodes,” Journal of the American Chemical Society, vol. 126, no. 38, pp. 11772-11773, Sep 29, 2004.
[7] V. S. Leite, and W. Figueiredo, “Spin-glass surface disorder on the magnetic behaviour of antiferromagnetic small particles,” Physica a-Statistical Mechanics and Its Applications, vol. 350, no. 2-4, pp. 379-392, May 15, 2005.
[8] T. Kaneyoshi, “Ferrimagnetic magnetizations of transverse Ising thin films with diluted surfaces,” Journal of Magnetism and Magnetic Materials, vol. 321, no. 21, pp. 3630-3636, Nov, 2009.
[9] M. Saber, I. Lukyanchuk, M. Madani, A. Tabyaoui, and A. Ainane, “The dielectric properties of the KH2PO4/KD2H2PO4 superlattice,” Chinese Journal of Physics, vol. 45, no. 1, pp. 58-74, Feb, 2007.
[10] I. Apostolova, and J. M. Wesselinowa, “Magnetic control of ferroelectric properties in multiferroic BiFeO3 nanoparticles,” Solid State Communications, vol. 147, no. 3-4, pp. 94-97, Jul, 2008.
[11] A. Lipinska, C. Simserides, K. N. Trohidou, M. Goryca, P. Kossacki, A. Majhofer, and T. Dietl, “Ferromagnetic properties of p-(Cd,Mn)Te quantum wells: Interpretation of magneto-optical measurements by Monte Carlo simulations,” Physical Review B, vol. 79, no. 23, Jun, 2009.
[12] E. Kantar, and M. Keskin, “Thermal and magnetic properties of ternary mixed Ising nanoparticles with core-shell structure: Effective-field theory approach,” Journal of Magnetism and Magnetic Materials, vol. 349, pp. 165-172, Jan, 2014.
[13] G. Salazar-Alvarez, J. Sort, A. Uheida, M. Muhammed, S. Surinach, M. D. Baro, and J. Nogues, “Reversible post-synthesis tuning of the superparamagnetic blocking temperature of gamma-Fe2O3 nanoparticles by adsorption and desorption of Co(II) ions,” Journal of Materials Chemistry, vol. 17, no. 4, pp. 322-328, 2007.

[14] L. Xi, Z. Wang, Y. Zuo, and X. N. Shi, "The enhanced microwave absorption property of CoFe2O4 nanoparticles coated with a Co3Fe7-Co nanoshell by thermal reduction," Nanotechnology, vol. 22, no. 4, Jan 28, 2011.
[15] J. H. Lee, I. N. Lund, E. T. Eisenbraun, and R. E. Geer, "Silicide-induced multi-wall carbon nanotube growth on silicon nanowires," Nanotechnology, vol. 22, no. 8, Feb 25, 2011.
[16] G. S. Chaubey, V. Nandwana, N. Poudyal, C. B. Rong, and J. P. Liu, "Synthesis and characterization of bimagnetic bricklike nanoparticles," Chemistry of Materials, vol. 20, no. 2, pp. 475-478, Jan 22, 2008.
[17] L. Wang, K. YuZhang, A. Metrot, P. Bonhomme, and M. Troyon, "TEM study of electrodeposited Ni/Cu multilayers in the form of nanowires," Thin Solid Films, vol. 288, no. 1-2, pp. 86-89, Nov 15, 1996.
[18] M. Chen, P. C. Searson, and C. L. Chien, "Micromagnetic behavior of electrodeposited Ni/Cu multilayer nanowires," Journal of Applied Physics, vol. 93, no. 10, pp. 8253-8255, May 15, 2003.
[19] L. Clime, S. Y. Zhao, P. Chen, F. Normandin, H. Roberge, and T. Veres, "The interaction field in arrays of ferromagnetic barcode nanowires," Nanotechnology, vol. 18, no. 43, Oct 31, 2007.
[20] Z. X. Song, Y. J. Xie, S. W. Yao, H. Z. Wang, W. G. Zhang, and Z. Y. Tang, "Microstructure and magnetic properties of electrodeposited Co/Cu multilayer nanowire arrays," Materials Letters, vol. 65, no. 11, pp. 1562-1564, Jun 15, 2011.
[21] L. Piraux, J. M. George, J. F. Despres, C. Leroy, E. Ferain, R. Legras, K. Ounadjela, and A. Fert, "Giant Magnetoresistance in Magnetic Multilayered Nanowires," Applied Physics Letters, vol. 65, no. 19, pp. 2484-2486, Nov 7, 1994.
[22] K. Liu, K. Nagodawithana, P. C. Searson, and C. L. Chien, "Perpendicular Giant Magnetoresistance of Multilayered Co/Cu Nanowires," Physical Review B, vol. 51, no. 11, pp. 7381-7384, Mar 15, 1995.
[23] R. Sharif, X. Q. Zhang, M. K. Rahman, S. Shamaila, J. Y. Chen, X. F. Han, and Y. K. Kim, "Fabrication and Magnetization Reversal Processes for Co/Cu Multilayer Nanowires," Ieee Transactions on Magnetics, vol. 45, no. 10, pp. 4033-4036, Oct, 2009.
[24] J. U. Cho, J. H. Min, S. P. Ko, J. Y. Soh, Y. K. Kim, J. H. Wu, and S. H. Choi, "Effect of external magnetic field on anisotropy of Co/Cu multilayer nanowires," Journal of Applied Physics, vol. 99, no. 8, Apr 15, 2006.
[25] S. Dubois, E. Chassaing, J. L. Duvail, L. Piraux, and M. G. Waals, "Preparation and characterization of electrodeposited Fe and Fe/Cu nanowires," Journal De Chimie Physique Et De Physico-Chimie Biologique, vol. 96, no. 8, pp. 1316-1331, Sep, 1999.
[26] K. Y. Kok, C. M. Hangarter, B. Goldsmith, I. K. Ng, N. B. Saidin, and N. V. Myung, "Synthesis and characterization of electrodeposited permalloy (Ni80Fe20)/Cu multilayered nanowires," Journal of Magnetism and Magnetic Materials, vol. 322, no. 24, pp. 3876-3881, Dec, 2010.
[27] X. T. Tang, G. C. Wang, and M. Shima, "Superparamagnetic behavior in ultrathin CoNi layers of electrodeposited CoNi/Cu multilayer nanowires," Journal of Applied Physics, vol. 99, no. 12, Jun 15, 2006.
[28] X. T. Tang, G. C. Wang, and M. Shima, "Layer thickness dependence of CPP giant magnetoresistance in individual CoNi/Cu multilayer nanowires grown by electrodeposition," Physical Review B, vol. 75, no. 13, Apr, 2007.
[29] P. Shakya, B. Cox, and D. Davis, "Giant Magnetoresistance and Coercivity of electrodeposited multilayered FeCoNi/Cu and CrFeCoNi/Cu," Journal of Magnetism and Magnetic Materials, vol. 324, no. 4, pp. 453-459, Feb, 2012.
[30] J. J. Park, M. Reddy, C. Mudivarthi, P. R. Downey, B. J. H. Stadler, and A. B. Flatau, "Characterization of the magnetic properties of multilayer magnetostrictive iron-gallium nanowires," Journal of Applied Physics, vol. 107, no. 9, May 1, 2010.
[31] Y. Peng, T. Cullis, G. Mobus, X. J. Xu, and B. Inkson, "Nanoscale characterization of CoPt/Pt multilayer nanowires," Nanotechnology, vol. 18, no. 48, Dec 5, 2007.
[32] H. P. Liang, Y. G. Guo, J. S. Hu, C. F. Zhu, L. J. Wan, and C. L. Bai, "Ni-Pt multilayered nanowire arrays with enhanced coercivity and high remanence ratio," Inorganic Chemistry, vol. 44, no. 9, pp. 3013-3015, May 2, 2005.
[33] P. Panigrahi, and R. Pati, "Tuning the ferromagnetism of one-dimensional Fe/Pt/Fe multilayer barcode nanowires via the barcode layer effect," Physical Review B, vol. 76, no. 2, Jul, 2007.
[34] M. Elawayeb, Y. Peng, K. J. Briston, and B. J. Inkson, "Electrical properties of individual NiFe/Pt multilayer nanowires measured in situ in a scanning electron microscope," Journal of Applied Physics, vol. 111, no. 3, Feb 1, 2012.
[35] S. Valizadeh, L. Hultman, J. M. George, and P. Leisner, "Template synthesis of Au/Co multilayered nanowires by electrochemical deposition," Advanced Functional Materials, vol. 12, no. 11-12, pp. 766-772, Dec, 2002.
[36] K. Qi, X. H. Li, H. Zhang, L. Wang, D. S. Xue, H. L. Zhang, B. F. Zhou, N. J. Mellors, and Y. Peng, "Nanoscale characterization and magnetic property of NiCoCu/Cu multilayer nanowires," Nanotechnology, vol. 23, no. 50, Dec 21, 2012.
[37] F. Nasirpouri, "Tunable Distribution of Magnetic Nanodiscs in an Array of Electrodeposited Multilayered Nanowires," Ieee Transactions on Magnetics, vol. 47, no. 8, pp. 2015-2021, Aug, 2011.
[38] M. Y. Rafique, L. Q. Pan, and A. Farid, "From nano-dendrite to nano-sphere of Co100-xNix alloy: Composition dependent morphology, structure and magnetic properties," Journal of Alloys and Compounds, vol. 656, pp. 443-451, Jan 25, 2016.
[39] V. Vega, T. Bohnert, S. Martens, M. Waleczek, J. M. Montero-Moreno, D. Gorlitz, V. M. Prida, and K. Nielsch, "Tuning the magnetic anisotropy of Co-Ni nanowires: comparison between single nanowires and nanowire arrays in hard-anodic aluminum oxide membranes," Nanotechnology, vol. 23, no. 46, Nov 23, 2012.
[40] P. Sirisangsawang, W. Rattanasakulthong, and S. Pinitsoontorn, "Composition dependence of structural,

morphological and magnetic properties of Co (FCC)-Cu granular films," International Journal of Physical Sciences, vol. 7 pp. 6044-6052, 2012.
[41] X. Lin, G. Ji, T. Gao, J. Nie, and Y. Du, "Magnetic properties of Co–Cu nanowire arrays fabricated in different conditions by SC electrodeposition," Solid State Communications, vol. 152, no. 16, pp. 1585-1589, 2012.
[42] C. Bran, E. M. Palmero, R. P. del Real, and M. Vazquez, "CoFeCu electroplated nanowire arrays: Role of composition and annealing on structure and magnetic properties," physica status solidi (a), vol. 211, no. 5, pp. 1076-1082, 2014.
[43] H. Z. Yang, M. Zeng, and R. H. Yu, "Magnetic properties of the NixCo1-x/Cu multilayer nanowires," Materials Research Bulletin, vol. 57, pp. 249-253, Sep, 2014.
[44] N. Zaim, A. Zaim, and M. Kerouad, "Monte Carlo study of the random magnetic field effect on the phase diagrams of a spin-1 cylindrical nanowire," Journal of Alloys and Compounds, vol. 663, pp. 516-523, 2016.
[45] M. Keskin, N. Sarli, and B. Deviren, "Hysteresis behaviors in a cylindrical Ising nanowire," Solid State Communications, vol. 151, no. 14-15, pp. 1025-1030, Jul-Aug, 2011.
[46] E. Kantar, "Hysteretic features of Ising-type segmented nanostructure with alternating magnetic wires," Journal of Alloys and Compounds, vol. 676, pp. 337-346, Aug 15, 2016.
[47] E. Kantar, and M. Ertas, "Influence of Frequency on the Kinetic Spin-3/2 Cylindrical Ising Nanowire System in an Oscillating Field," Journal of Superconductivity and Novel Magnetism, vol. 28, no. 8, pp. 2529-2538, Aug, 2015.
[48] E. Kantar, and M. Ertas, "Cylindrical Ising nanowire in an oscillating magnetic field and dynamic compensation temperature," Superlattices and Microstructures, vol. 75, pp. 831-842, Nov, 2014.
[49] M. Ertas, and E. Kantar, "Cylindrical Ising nanowire with crystal field: existence of a dynamic compensation temperatures," Phase Transitions, vol. 88, no. 6, pp. 567-581, Jun 3, 2015.
[50] A. Feraoun, A. Zaim, and M. Kerouad, "Monte Carlo study of a mixed spin (1,3/2) ferrimagnetic nanowire with core/shell morphology," Physica B-Condensed Matter, vol. 445, pp. 74-80, Jul 15, 2014.
[51] E. Kantar, M. Ertas, and M. Keskin, "Dynamic phase diagrams of a cylindrical Ising nanowire in the presence of a time dependent magnetic field," Journal of Magnetism and Magnetic Materials, vol. 361, pp. 61-67, Jun, 2014.
[52] B. Deviren, E. Kantar, and M. Keskin, "Dynamic phase transitions in a cylindrical Ising nanowire under a time-dependent oscillating magnetic field," Journal of Magnetism and Magnetic Materials, vol. 324, no. 13, pp. 2163-2170, Jul, 2012.
[53] E. Kantar, and Y. Kocakaplan, "Hexagonal type Ising nanowire with mixed spins: Some dynamic behaviors," Journal of Magnetism and Magnetic Materials, vol. 393, pp. 574-583, Nov 1, 2015.
[54] E. Kantar, "Composition, temperature and geometric dependent hysteresis behaviours in Ising-type segmented nanowire with magnetic and diluted magnetic, and its soft/hard magnetic characteristics," Philosophical Magazine, vol. 97, no. 6, pp. 431-450, 2017.
[55] E. Kantar, "Geometry-Dependent Magnetic Properties of Ising-Type Multisegment Nanowires," Journal of Superconductivity and Novel Magnetism, vol. 29, no. 10, pp. 2699-2704, Oct, 2016.
[56] T. Kaneyoshi, I. P. Fittipaldi, R. Honmura, and T. Manabe, "New Correlated-Effective-Field Theory in the Ising-Model," Physical Review B, vol. 24, no. 1, pp. 481-484, 1981.
[57] J.W. Tucker, "Generalized Van der Waerden identities," Journal of Physics A: Mathematical and General, vol. 27, pp. 659 1994.
[58] Y. Kocakaplan, E. Kantar, and M. Keskin, "Hysteresis loops and compensation behavior of cylindrical transverse spin-1 Ising nanowire with the crystal field within effective-field theory based on a probability distribution technique," European Physical Journal B, vol. 86, no. 10, Oct 7, 2013.
[59] H. Magoussi, A. Zaim, and M. Kerouad, "Monte Carlo simulation of the magnetic properties of a spin-1 Blume-Capel nanowire," Solid State Communications, vol. 200, pp. 32-41, Dec, 2014.
[60] H. Magoussi, A. Zaim, an M. Kerouad, "Magnetic properties of a nanoscaled ferrimagnetic thin film: Monte Carlo and effective field treatments," Superlattices and Microstructures, vol. 89 pp. 188-203, 2016.
[61] M. El Hamri, S. Bouhou, I. Essaoudi, A. Ainane, and R. Ahuja, "Magnetic properties of a diluted spin-1/2 Ising nanocube," Physica a-Statistical Mechanics and Its Applications, vol. 443, pp. 385-398, Feb 1, 2016.
[62] J. S. Suen, M. H. Lee, G. Teeter, and J. L. Erskine, "Magnetic hysteresis dynamics of thin Co films on Cu(001)," Physical Review B, vol. 59, no. 6, pp. 4249-4259, Feb 1, 1999.
[63] H. W. Wu, C. J. Tsai, and L. J. Chen, "Room temperature ferromagnetism in Mn+-implanted Si nanowires," Applied Physics Letters, vol. 90, no. 4, Jan 22, 2007.
[64] S. Ishrat, K. Maaz, K. J. Lee, M. H. Jung, and G. H. Kim, "Fabrication and temperature-dependent magnetic properties of one-dimensional embedded nickel segment in gold nanowires," Journal of Alloys and Compounds, vol. 541, pp. 483-487, Nov 15, 2012.